INTERNATIONAL JOURNAL OF
COASTAL & OFFSHORE ENGINEERING
IJCOE Vol.5/No. 2/Summer 2020 (23-40)

Available online at: www. Ijcoe.org

Application of tuned liquid column damper for motion reduction of semisubmersible platforms

Hamidreza Feizian[1], Mehdi Shafieefar[2*], Roozbeh Panahi[3]

[1]*PhD Student, Faculty of Civil and Environmental Engineering, Tarbiat Modares University; h.feizian@modares.ac.ir*
[2]*Professor, Faculty of Civil and Environmental Engineering, Tarbiat Modares University; shafiee @modares.ac.ir*
[2]*Assistant Professor, Faculty of Civil and Environmental Engineering, Tarbiat Modares University; rpanahi @modares.ac.ir*

ARTICLE INFO

Article History:
Received: 27 May. 2020
Accepted: 21 Dec. 2020

Keywords:
Tuned liquid column damper;
Semisubmersible platform;
Low-frequency motion;
Irregular waves

ABSTRACT

Incorporation of a tuned liquid column damper (TLCD) into a semisubmersible drilling platform is numerically investigated in this paper. First, a governing equation for liquid fluctuation in the TLCD is derived for the planar motion of the TLCD in conjunction with the motion of the platform. Then, the real-time response of the platform under irregular waves is analyzed using radiation/diffraction theory in which TLCD loading is exerted on the platform at each time-step. This facilitates capture of the difference-frequency and sum frequency second order wave forces and the low-frequency motion of the platform. The results show that the effect of the rotational motion of the platform on the TLCD is significant and the TLCD has a reciprocal effect on this rotational motion of the platform. It is shown that the TLCD decreases the low-frequency motion of the platform and has no considerable effect on the wave-frequency motion. Also, the sensitivity of the platform motion to the main specifications of the TLCD is assessed by a parametric study.

1. Introduction

Offshore floating platforms are employed worldwide for various deep-water applications. It is essential to control the motion and vibration of such platforms in order to maintain safety and comfort of personals. Thus, researchers have implemented different approaches to reduce motion of floating platforms. Structural shape optimization has been investigated by Clauss and Birk [1], Adjami and Shafieefar [2], Lee and Lim [3], Muskulus and Schafhirt [4] and Hall et al. [5]. However, this approach is not applicable to the existing platforms because it remains in the conceptual design stage.

Mooring optimization is another effective approach for motion reduction of existing platforms. Shafieefar and Rezvani [6] optimized the mooring pattern, length and tension for a ship-shaped floating platform using a genetic algorithm (GA). A GA was also used by Mirzaei [7] to optimize the mooring pattern of a crane barge. Ren et al. [8] studied the effect of additional mooring chains on the motion of a floating wind turbine with a tension leg platform. Brommundt et al. [9] worked on floating wind turbines using a simplex algorithm to determine the optimum line configuration for a semisubmersible platform.

Passive methods such as a tuned mass damper (TMD) and tuned liquid column damper (TLCD) have been increasingly considered for offshore fixed and floating platforms [10]. The TLCD is the most attractive of these approaches because of its low cost, ease of handling, and limited maintenance requirements [11,12]. TLCDs have been used for many years for fixed structures on land, such as for buildings with short periods [13–17]. It should be noted that the hydrodynamics of moored floating structures with very long periods differ from the dynamics of fixed structures on land.

A TLCD is a U-shaped tube containing a liquid (commonly water) which has an orifice that usually is located in the middle of the tube. While the liquid oscillates in the tube, the orifice causes head loss, resulting in energy dissipation. The blocking ratio of the orifice, the natural frequency of the fluctuation of the liquid in the damper (natural frequency of the TLCD) and the mass of the TLCD are parameters that affect the efficiency of the damper. These parameters should be tuned properly in consideration of the dynamic specifications of the main structure [18].

Using a numerical method, Lee et al. [19] studied a typical tension leg platform (TLP) with a TLCD on its deck in order to decrease the wave-

induced 2D motion of the platform. Their parametric analysis considered the pontoon diameter, pontoon draft, and the total mass of the platform, but overlooked changes in the TLCD parameters. They used the well-known equation of motion for liquid in a TLCD (governing equation) presented by Sakai et al. [20]. This equation is derived for a TLCD moving in a single horizontal direction, although floating platforms tend to experience vertical and rotational motions. They focused on surge motion and stated that the optimum natural frequency of the TLCD is equal to the surge natural frequency of the platform. However, floating platforms commonly experience low natural frequencies and a TLCD would have to be much wider than the platform in order to have the same frequency [21].

A TLP equipped with an underwater TLCD (UWTLCD) was studied experimentally by Lee and Juang [22]. The columns of the platform were used as the vertical parts of the TLCD and were connected by a small-diameter horizontal tube. Thus, the platform was equipped with a TLCD that did not occupy space on the deck. The effectiveness of the UWTLCD was investigated for the surge, heave and pitch motions in regular waves. The pontoon draft, tether pretension force and liquid length in the TLCD, which affects its mass and natural frequency, were considered in their parametric study.

Coudurier et al. [23] proposed a tuned liquid multi-column damper (TLMCD) to dissipate the energy of waves having various angles of incidence. They numerically applied the proposed damper to a barge-type floating wind turbine by focusing on rotational motion. The natural frequency of the damper was tuned to the same roll/pitch natural frequency of the barge platform. The optimized blocking ratio of the orifice was calculated for an arbitrary mass of the damper at a constant wave height.

In the present study, application of a TLCD for a large floating platform (GVA4000 semisubmersible) with long natural periods is investigated numerically and surge, heave and pitch motions of the platform are studied. Since the real-time response of the platform in irregular waves is calculated, the difference-frequency wave forces are included as well as the wave frequency forces. Thus, the low-frequency and wave-frequency motions of the platform are considered. Capturing the low-frequency motions of floating platforms is an important issue which is not considered in the previous studies. This would cause ignoring some important phenomena in platform motions. A more complete form of the governing equation of liquid fluctuation in the TLCD is derived in section 2, which takes into consideration the effects of transitional and rotational motion of the platform.

Since there is no experimental data available for application of a TLCD on a large semisubmersible such as the GVA4000, first, the case study platform is simulated without a damper. The Results are used in section 3 to verify the numerical modeling by comparing the simulation results with the available experimental data. Then, the platform-TLCD system is simulated and a parametric study is carried out to consider the performance of applying TLCD for reducing the platform motions. Results of the platform-TLCD system responses are discussed in section 4. The natural frequency, blocking ratio of the orifice and mass ratio of the TLCD are the study parameters. Section 5 presents the conclusions.

2. Governing equations of liquid fluctuation in TLCD and generated loads

There are two approaches for mathematical modeling of a structure with TLCD system. In the first approach, the whole system is considered as a single unit and the equation of motion for the structure and damper is derived simultaneously, as done by Holden et al. [24]. In the second method, motion of the main structure is calculated using an appropriate numerical model and the TLCD-induced forces are computed separately and applied to the structure [25,26]. The first method derives and solves the equation of motion of a coupled system for any type of structure. Because dynamics of various types of fixed and floating structures are complicated, it is better to solve the equation of liquid fluctuation inside the damper separately. The damper-induced forces can be calculated for exertion on the structure using the second method.

Hochrainer [27] introduced a method to derive the governing equation of liquid motion in a U-shaped TLCD (Fig. 1) for the transitional motion of the damper in the horizontal (X) and vertical (Z) directions as follows:

$$L_{eq}\ddot{w} + \frac{1}{2}\xi\dot{w}|\dot{w}| + 2gw = -B.\ddot{X} - \ddot{Z}(2w) \tag{2.1}$$

where, w, $\dot{w}$ and $\ddot{w}$ denote the magnitudes of liquid displacement, velocity and acceleration in the vertical parts of the tube, respectively, and $\ddot{X}$ and $\ddot{Z}$ are the magnitudes of horizontal and vertical acceleration of the damper. The positive direction for liquid motion is assumed to be from left to right in the horizontal tube (as the liquid surface moves down in the left vertical tube and moves up in the right one) . As shown in Fig. 1, B and A_h are the length and cross-section area of the horizontal tube, A_v is the cross-section area of the vertical tubes, H is the initial height of the liquid in the vertical tubes and L is the total length of the liquid in the tube ($L = 2H + B$).

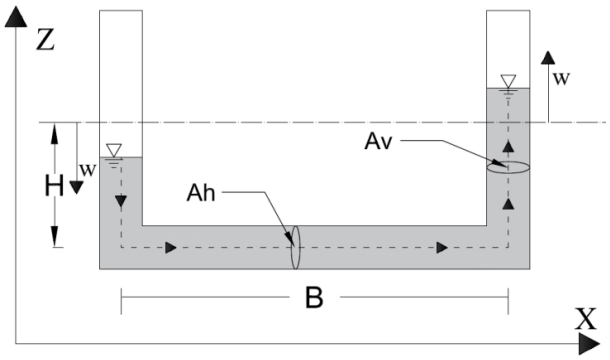

Fig. 1. U-Shaped TLCD with transitional motion.

Finally, L_{eq} is defined as:

$$L_{eq} = L - B\left(1 - \frac{A_v}{A_h}\right) \tag{2.2}$$

Parameter ξ is the head loss coefficient of the TLCD and is related to the blocking ratio of the orifice (ratio of the area enclosed by the orifice to the total area of the horizontal tube) calibrated from the experiment results. Wu et al. [18] calibrated this coefficient by conducting forced harmonic vibration tests for uniform sections of TLCDs of various dimensions and blocking ratios as summarized in Table 1.

They concluded that ξ is not a function of TLCD natural frequency, but is mainly related to the blocking ratio. They proposed a formula for calculating ξ as a function of blocking ratio [18] as:

$$\xi = (-0.6\psi + 2.1\psi^{0.1})^{1.6}(1-\psi)^{-2} \tag{2.3}$$

where ψ is the blocking ratio of the orifice inside the damper.

Table 1. Calibration tests results for head loss coefficient of TLCD [18]

Blocking ratio (ψ)	Natural frequency (Hz)			
	0.4923	0.4727	0.4595	0.4516
	Head loss coefficient: (ξ)			
20%	3.96	3.55	3.40	3.40
40%	6.10	5.80	5.70	5.55
60%	12.80	12.40	12.50	12.00
80%	54.50	54.00	59.00	56.00

The rotational motion of the TLCD is extensively studied by Xue et al. [28]; Suduo et al. [29] and Taflanidis et al. [30]. For a TLCD rotating around a fixed point, the governing equation of liquid fluctuation is [28]:

$$L_{eq}\ddot{w} + \frac{1}{2}\xi\dot{w}|\dot{w}| + 2gw = -B\left(\ddot{\theta}\left((L-B)/2 + D\right) + g\theta\right) \tag{2.4}$$

in which θ and $\ddot{\theta}$ denote the magnitudes of rotating angle and rotational acceleration, respectively, and D is the distance of the horizontal tube of the TLCD from the rotating center (Fig. 2).

The governing equation of liquid fluctuation in a TLCD is often derived for a moving system with a single degree of freedom. A semisubmersible platform may has large displacement at all degrees of freedom (DOF) [31]. Therefore, when using a TLCD on this type of structure, it is important to derive the governing equation such that the effects of all motions are taken into account. For the combined rotation and transition of the TLCD, the superposition principle cannot be used because of the nonlinear behavior of the liquid fluctuation inside the damper. Thus, the governing equation for a damper experiencing simultaneous transitional and rotational motions should be derived exclusively.

Coudurier et al. [23] presented TLCD equations for combined transition and rotation; however, their equations were derived in a complicated format which does not clearly represent the physical process and is very difficult to compare with well-known equations in the literature. The equations are also difficult to apply.

The formulation proposed in the current study is derived in a simple format that is analogous to the well-known form presented in the literature. When applying a TLCD to a floating structure, coordinate system *XOZ* is considered to be fixed on a water free surface as shown in Fig. 2. The floating body is defined using its center of mass (*G*) and 3 DOF (*X*, *Z* and θ) with a TLCD attached to the floating body. Assuming that the energy of the liquid remains constant during the motion of the TLCD, the Lagrange equation can be applied as follows [32]:

$$\frac{d}{dt}\left(\frac{\partial(T-U)}{\partial\dot{w}}\right) - \frac{\partial(T-U)}{\partial w} = Q \tag{2.5}$$

where U and T are the potential and kinetic energy of the liquid, respectively, and Q represents the magnitude of non-conservative force acting on the liquid in the following form [32]:

$$Q = -\frac{1}{2}\rho r A_v \xi \dot{w}|\dot{w} \tag{2.6}$$

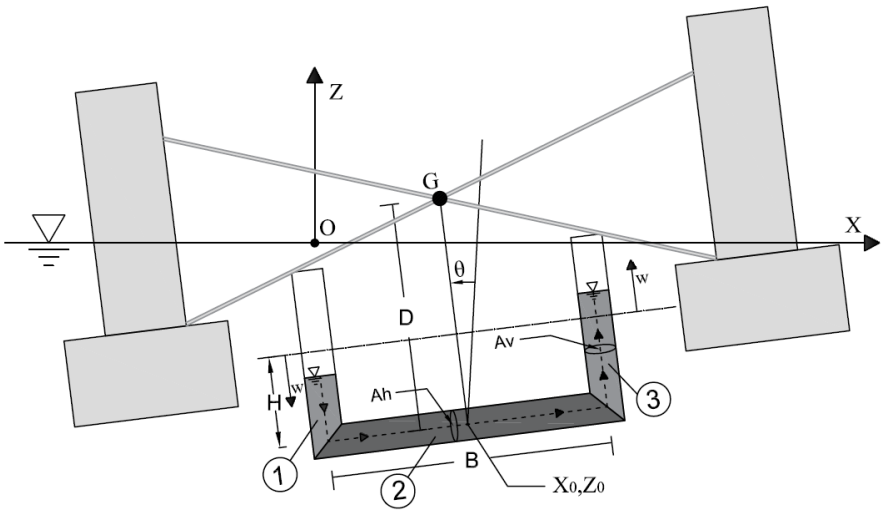

Fig. 2. U-Shaped TLCD attached to floating platform experiencing combined rotation and transition.

For relatively small rotation angles ($\theta < 10°$), $\cos(\theta)$ and $\sin(\theta)$ are estimated to be 1 and θ, respectively, $[\cos(\theta)\sim 1\ ,\ \sin(\theta)\sim\theta]$. In order to calculate the kinetic energy of the liquid ($T = 1/2.\,\mathrm{m}V^2$), the magnitudes of total velocities along the vertical and horizontal tubes can be written as follow for the three portions of the damper:

$$V_1 = \dot{w} + \frac{\dot{\theta}B}{2} + \dot{X}\theta - \dot{Z} \tag{2.7}$$

$$V_2 = r\dot{w} + \dot{\theta}D + \dot{X} + \dot{Z}\theta \tag{2.8}$$

$$V_3 = \dot{w} + \frac{\dot{\theta}B}{2} - \dot{X}\theta + \dot{Z} \tag{2.9}$$

in which r denotes the ratio of A_v to A_h ($r = A_v/A_h$) and $\dot{X}$ and $\dot{Z}$ denote the magnitudes of horizontal and vertical velocities of the structure. The average heights of the three portions of the TLCD, according to the potential energy of the liquid ($U = mgZ$), can be defined as:

$$Z_{ave,1} = Z_0 - \frac{B}{2}\theta + \frac{1}{2}(H - w) \tag{2.10}$$

$$Z_{ave,2} = Z_0 \tag{2.11}$$

$$Z_{ave,3} = Z_0 + \frac{B}{2}\theta + \frac{1}{2}(H + w) \tag{2.12}$$

By calculating the kinetic and potential energy of the damper liquid and substituting these values into Eq.(2.5), the governing equation of liquid motion in TLCD becomes:

$$L_{eq}\ddot{w} + \frac{1}{2}r\xi\dot{w}|\dot{w}| + 2gw = \left[-B.\ddot{X}\right] + \left[-\ddot{Z}(2w)\right] + \left[-B\left(\ddot{\theta}\left(\frac{(L-B)}{2} + D\right) + g\theta\right)\right] + \left[-\ddot{Z}B\theta + 2w\ddot{X}\theta + 2w\dot{X}\dot{\theta} - B\dot{\theta}\dot{X}\theta\right] \tag{2.13}$$

X-term *Z-term* *θ-term* *Additional terms*

This equation describes liquid fluctuation in a TLCD as the result of the simultaneous motion at all 3 DOF. For purely transitional movement of the damper, all terms containing θ should be omitted from Eq.(2.13), which then becomes the Eq.(2.1) as previously derived for damper transition. Similarly, for purely rotational movement of the damper, all terms containing X and Z should be omitted from Eq.(2.13), which then becomes the Eq.(2.4). The equation derived here has a form that is similar to previously derived equations; thus, its validity can be demonstrated by comparing with equations that are verified in previous studies.

The right-hand side of Eq.(2.13) shows that the first three terms are the components of TLCD motion at 3 DOF. These three terms are related to pure structure motions in the X (surge), Z (heave) and θ (pitch) directions, respectively. These are denoted as the X-term, Z-term and θ-term, respectively. There are four additional terms on the right-hand side of Eq.(2.13) which are the results of simultaneous motion of the dampers at 3 DOF and are denoted as "additional terms". The magnitudes of these seven terms will determine the effects of structural motions on TLCD excitation and are denoted as "excitation terms". Section 4 compares the magnitude and effect of each term on damper efficiency for the specified conditions.

The natural frequency of the TLCD is an important characteristic of this damper and can be estimated as [12]:

$$f_{TLCD} = \frac{1}{2\pi}\sqrt{\frac{2g}{L_{eq}}} = \frac{1}{2\pi}\omega_{TLCD} \tag{2.14}$$

The main structural dimensions limit the total equivalent length of the liquid in the damper (L_{eq}) and

prevent the setting of an arbitrary value for it. The tuning ratio equals $f_{TLCD}/f_{Structure}$ and an appropriate quantity for this ratio is 0.95 to 1.05 [12,19].

The loads generated by the TLCD can be calculated as [25, 26]:

$$F_X = -\rho A_h B\ddot{w} - \rho(A_h B + 2HA_v)\ddot{X} \tag{2.15}$$

$$F_Z = -\rho(2A_v w\ddot{w}) - \rho(A_h B + 2HA_v)\ddot{Z} \tag{2.16}$$

$$M_\theta = -\rho A_v B\left(\frac{(L-B)}{2} + D\right)\ddot{w} - \rho g A_v\left(\left((\mathrm{L}-\mathrm{B}) + B\frac{A_h}{A_v}\right)D\theta + Bw\right) - I_d\ddot{\theta} \tag{2.17}$$

where $\boldsymbol{F_X}$, $\boldsymbol{F_Z}$ and $\boldsymbol{M_\theta}$ are the magnitudes of forces exerted on the mass-center of the platform by the TLCD in the *X, Z* and θ directions, respectively, and $\boldsymbol{I_d}$ is the moment of inertia of the damper liquid about the mass center *G*. Other parameters have been defined previously. It is important to note that these equations have been updated for a non-uniform TLCD cross-section.

3. Numerical modeling

Characteristics of a GVA4000 drilling semisubmersible are used to model the effects of a TLCD on its response mitigation by considering available experimental data for hydrodynamic motion of the platform [33]. This semisubmersible platform has already been tested using a 1:81 scale model by Clauss et al. [33] to calculate its RAOs for the heave and pitch motions. The main dimensions and characteristics of the platform model are shown in Fig. 3 and Table 2.

Numerical modeling is carried out in two stages. The hydrodynamic specifications of the platform are determined at the frequency-domain stage. This is followed by the time-domain stage in which platform motions are determined under the influence of irregular waves. Then, the forces and moment induced by the TLCD are calculated and applied to the structure using Eqs. (2.15) to (2.17). The motions are determined by ANSYS-AQWA (17.0) at each time-step and the related TLCD loads are applied to the platform using a Fortran code in an external dynamic library link file. This Fortran code solves the governing equation of the TLCD (Eq.(2.13)) at each time-step using the Newmark-beta method [34] and then calculates the damper forces.

Accuracy of numerical modeling of the platform (without TLCD) is confirmed by comparing the results with available experimental data.

However, since there is no any experimental data available on application of a TLCD to a large semisubmersible, the validity of the new derived Eq.(2.13) is investigated by comparing it with Eq.(2.1) and Eq.(2.4) which are validated several times in the literature.

Table 2. Characteristics of GVA4000 model

Structure characteristics	Value
Mass center *X* (m)	0
Mass center *Y* (m)	0
Mass center *Z* (m)	0.85
Mass (kg)	25834154
K_{xx}, K_{yy}, K_{zz} (m)	30.4, 31.06, 37.54
Water depth (m)	121
Mooring line length (m)	400
Mooring line density (kg/m)	140
Mooring line stiffness *EA* (kN)	500000
Natural frequencies f_{surge}, f_{heave}, f_{pitch} (results of decay test models)	0.008, 0.046, 0.015

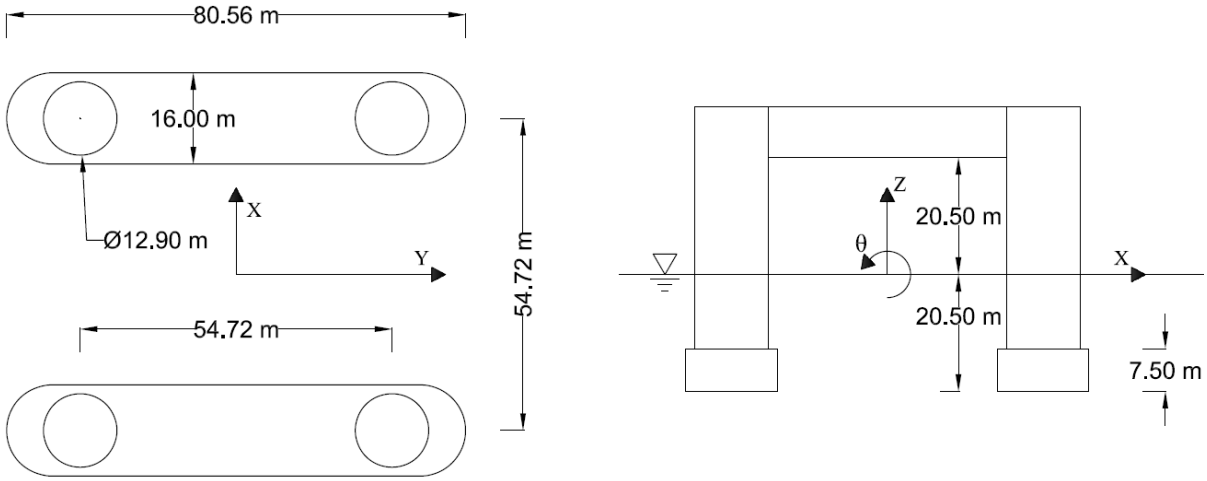

Fig. 3. Main dimensions of GVA4000 platform [33]

3.1. Frequency-domain analysis without TLCD

ANSYS-AQWA employs a combination of the Morison's equation for slender elements (Morison's elements) and the radiation/diffraction theory for large ones. It calculates the fluid velocity potential based on the following assumptions [35]:

- The body has zero or slight forward speed.
- The fluid is inviscid and incompressible and the fluid flow is irrotational.
- The incident regular wave train is of small amplitude compared to its length (small slope).
- The motions are first-order and must be of small amplitude.

The velocity potential is composed of the incident, diffracted and radiated waves of the floating structure and has the following form:

$$\varphi(\vec{X})e^{-i\omega t} = \left[(\varphi_I + \varphi_d) + \sum_{j=1}^{6} \varphi_{rj} x_j\right] e^{-i\omega t} \quad (3.1)$$

where φ_I is the first-order incident wave potential at unit wave amplitude, φ_d is the corresponding diffracted wave potential, φ_{rj} is the radiation wave potential due to the j^{th} motion at unit amplitude and x_j is the motion amplitude of the j^{th} DOF excited by an incident regular wave at unit amplitude [35].

The radiation potential results in pressure fields and forces on the surface of the floating body. The component of the forces that is in phase with the body velocity acts as a damping term and the out-of phase component which is in phase with the body acceleration acts as an inertia term. This component is called the added mass term [36].

The Morison's equation also includes a force component due to body acceleration which contributes to the total added mass. The other force component in the Morison's equation is in phase with the body velocity. The latter one is called the drag force.

Using the aforementioned theory, ANSYS-AQWA (17.0) is applied to calculate the platform RAOs. Then, the calculated RAOs are compared with the experimental data given by Clauss et al. [33] as represented in Fig. 4 and Fig. 5. A qualitative comparison shows that the present numerical results match well with the experimental data. The frequency domain results show that the numerical model is capable of calculating the platform motion with acceptable precision. Section 4 discusses the application of the TLCD to the modeled semisubmersible platform.

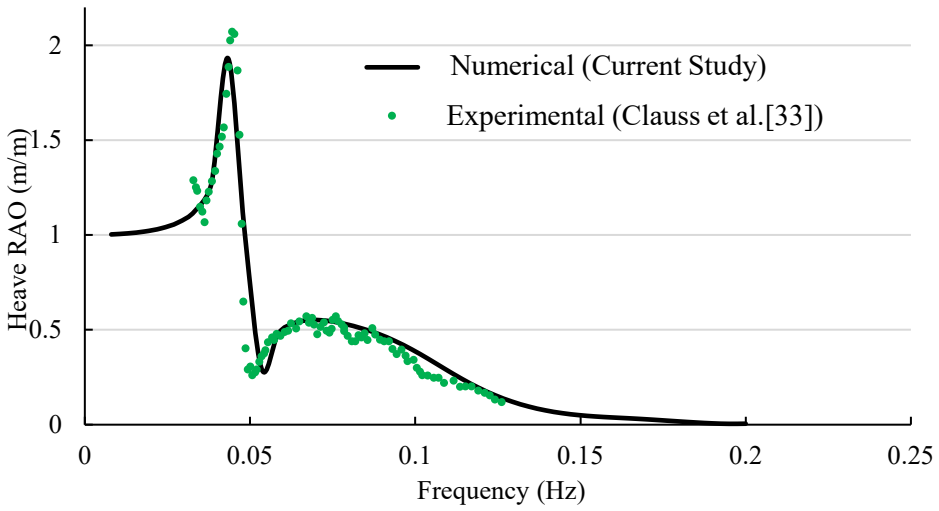

Fig. 4. Comparison of heave RAO for current study and Clauss et al. [33].

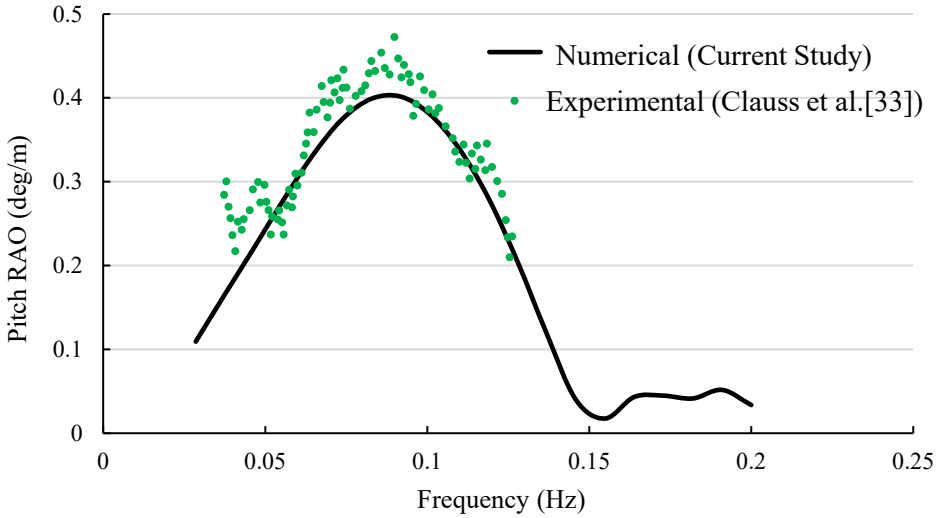

Fig. 5. Comparison of pitch RAO for current study and Clauss et al. [33]**.**

3.2. Time domain analysis with TLCD

ANSYS AQWA is capable to simulate the real-time motion of a floating body under irregular waves. Wave-frequency motions and low period oscillatory drift motions may be considered. The difference-frequency and sum frequency second order forces are calculated at each time step in the simulation, together with the first order wave frequency forces and instantaneous values of all other forces. This, can also provide calculating wave drift damping which is induced by nonlinear surface wave effects [37].

The configurations used to investigate the influence of the TLCD on response of the semisubmersible platform are summarized in Table 3. In each study condition, two TLCDs are mounted on the platform in which their vertical tubes are located inside the platform's columns (Fig. 9). The head loss coefficient, natural frequency and mass ratio ($M_{TLCD\ Fluid}/M_{Structure}$) are examined as the main variables that affect platform motion. Different values for parametric analysis are set for each variable while keeping the other two variables constant. The dimensions of the TLCD are determined by considering the GVA4000 hull dimensions. In all models, the damper width is 55 m and the total length of the liquid in the tube is 85 m with a density of 1000 kg/m^3.

Table 3. TLCD configurations in parametric analysis

Selected specification of TLCD for parametric study	A_v (m^2)	A_h (m^2)	f_n(Hz) [T (s)]	Mass ratio (%)	Head loss coefficient (ξ)
Head loss coefficient (ξ)	2×5.10 (D = 2.55)		0.077 [13.07]	3.44	3.50 5.50 12.50 55.00
Natural frequency (period)	2×5.10 (D_v = 2.55) 2×7.54 (D_v = 3.1) 2×10.17 (D = 3.6)	2×5.10 (D_h = 2.55) 2×3.46 (D_h = 2.1) 2×1.77 (D = 1.5)	0.077 [13.07] 0.058 [17.36] 0.038 [26.41]	3.44	55.00
TLCD /Structure mass ratio	2×0.126 (D = 0.4) 2×1.77 (D = 1.5) 2×3.46 (D = 2.1) 2×9.62 (D = 3.5) 2×12.56 (D = 4.0) 2×15.90 (D = 4.5) 2×19.62 (D = 5.0) 2×23.75 (D = 5.5) 2×28.26 (D = 6.0)		0.077 [13.07]	0.08 1.2 2.3 6.49 8.47 10.72 13.24 16.02 19.06	55.00

Similar to results of Wu et al. [18], the head loss coefficient of the damper is estimated to be 3.5 to 55 for blocking ratios of 20% to 80%. The largest structure-TLCD mass ratio is 19%, which is a large ratio for liquid dampers. An extremely small value of 0.08% is selected to investigate the extreme condition. The natural frequency of the TLCD is varied from 0.038 to 0.077Hz because of the restrictions related to

the structural dimensions. It is not possible to tune the structure-TLCD frequency ratio to approach 1 as recommended in previous studies. The natural frequency of the platform is estimated by conducting decay test models. Because mooring lines stiffness would affect the natural frequency of the platform, using the timed domain modelling which is capable to capture the mooring lines dynamics is preferred. For the surge, heave and pitch motions, the natural frequencies of the platform are calculated to be 0.008, 0.046 and 0.015 Hz, respectively. The results of the decay tests are shown in Fig. 6 to Fig. 8.

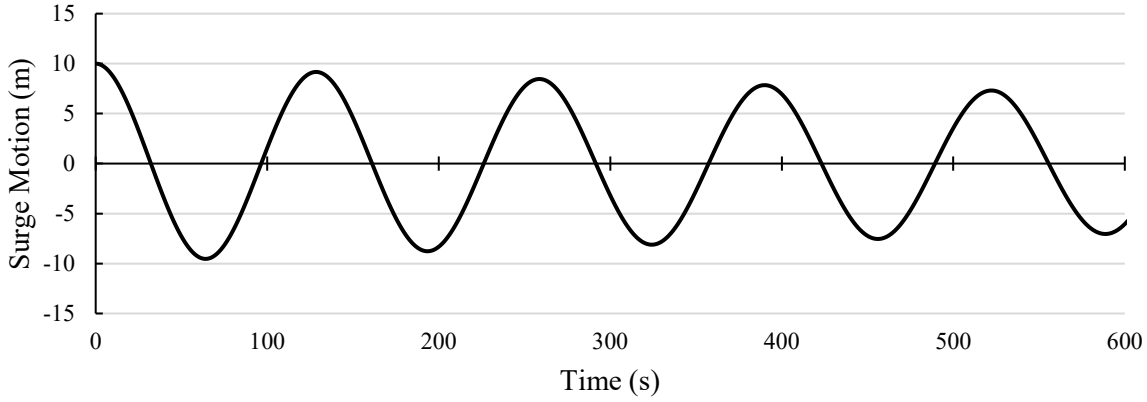

Fig. 6. Decay test model results for surge motion of GVA4000 platform (without TLCD)

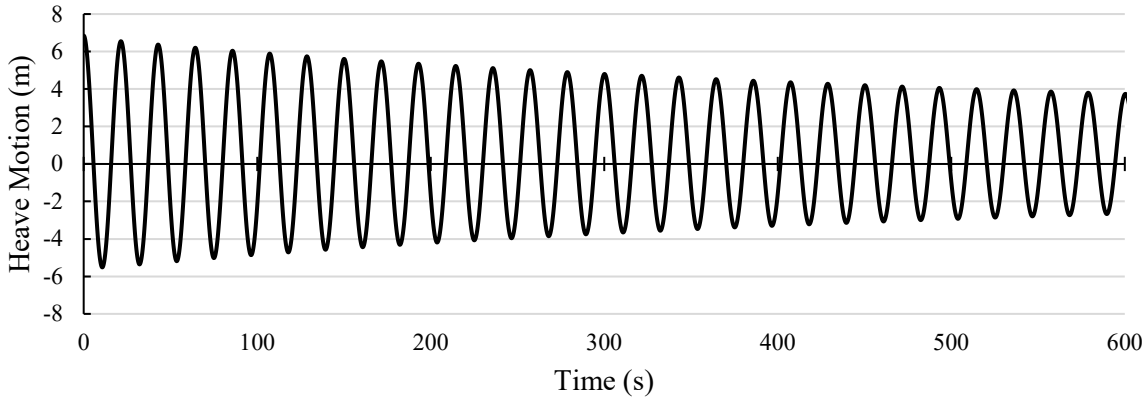

Fig. 7. Decay test model results for heave motion of GVA4000 platform (without TLCD)

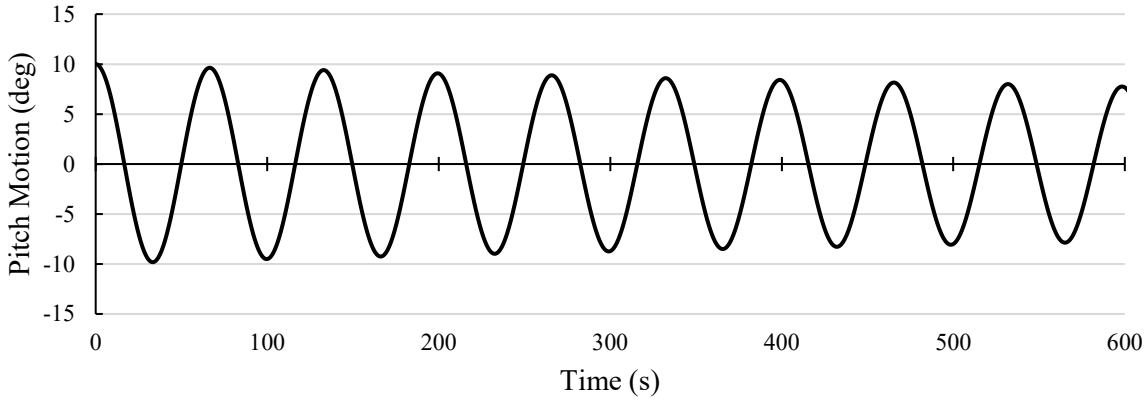

Fig. 8. Decay test model results for pitch motion of GVA4000 platform (without TLCD)

Time series of irregular waves with significant wave height of 5 m (H_s = 5 m) and peak frequency of 0.09 Hz (T_p = 11 s) is generated based on the JONSWAP spectrum. A schematic view of TLCD placement onto a GVA4000 semisubmersible is shown in Fig. 9. In this figure global directions of reference coordinate axes are defined. But it should be considered that the precise definition of reference coordinates is shown in Fig. 2. It is assumed that the waves are propagating in X direction. The selected sea state is related to the 1-

year return period wave characteristics in the Caspian sea which is applied as the operational condition as recommended by API [38]. The time series of the water surface elevation for the sea state is shown in Fig. 9

In time-domain analysis, ANSYS-AQWA facilitates the use of additional formulations through the dynamic link library (DLL). This feature is used to introduce the external loads exerted by the TLCD at each time-step using the external DLL built from the Fortran code. The code determines the platform position and velocity as inputs, calculates the TLCD forces and presented them to ANSYS-AQWA as external forces to be exerted on the platform. The positions and velocities of the platform are determined at each time-step by integrating the accelerations from all hydrodynamic and TLCD forces.

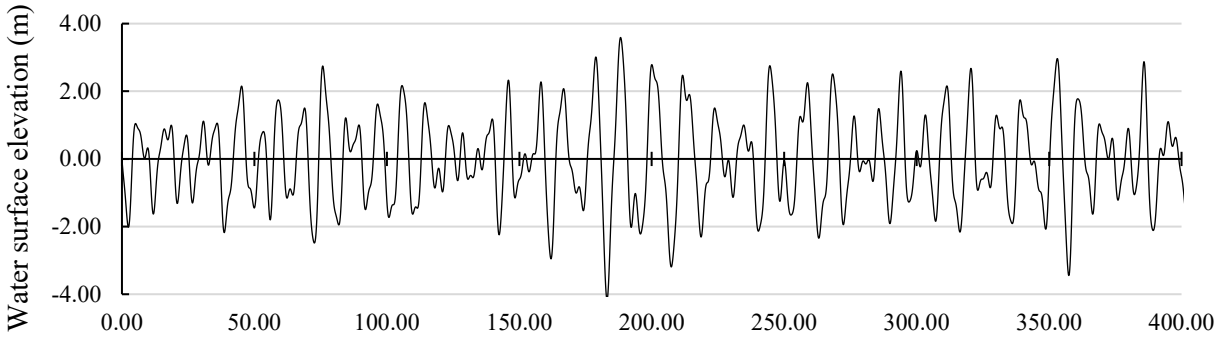

Fig. 9. Water surface elevation of the selected sea-state (Hs=5 m, Tp=11 s)

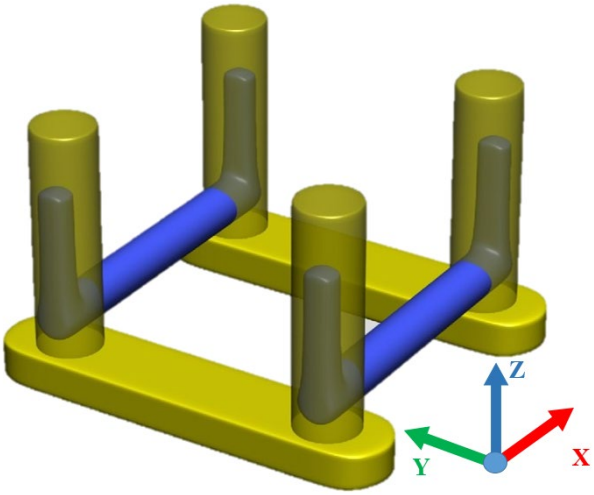

Fig. 10. Schematic view of TLCD on GVA4000 semisubmersible floating platform.

4. Results and discussion

Time-domain analysis of the floating platform response is carried out with and without the TLCD in different configurations as shown in Table 3. However, for better evaluation of the results, all response time histories are transformed into frequency domain by the fast Fourier transform[1] method. It is evident from the modeling results that the dynamic energy of the structure is concentrated at two frequency ranges for 3 DOF. Fig. 10 to Fig. 12 show a major peak near the natural frequency of the platform in each direction and a smaller peak close to the peak wave frequency. The major peak is the result of the difference-frequency forces of the irregular waves, which cause resonance in the natural frequency of the platform as described by Keddam [39]. This peak is about 100 times higher than that of the minor peaks for surge. But for heave and pitch motions the values of the two peaks are close together.

[1] FFT

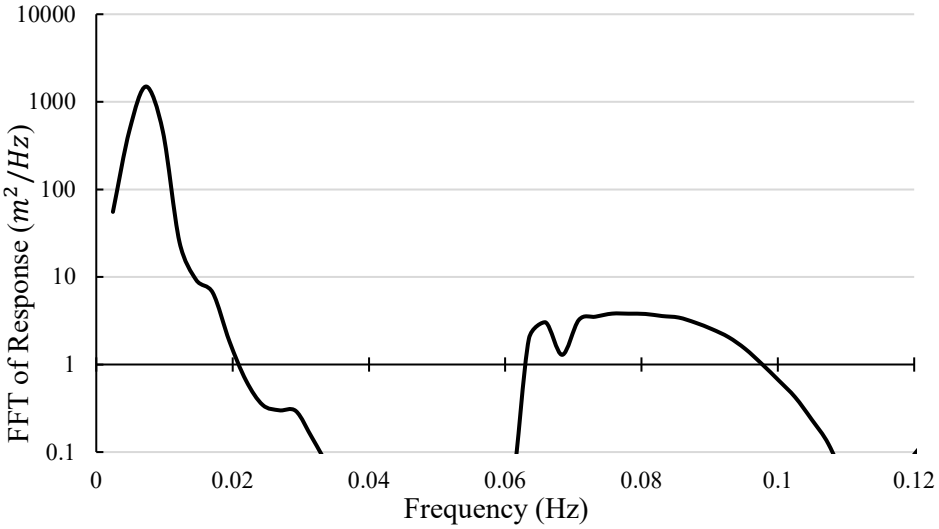

Fig. 11. Surge response without TLCD (logarithmic scale).

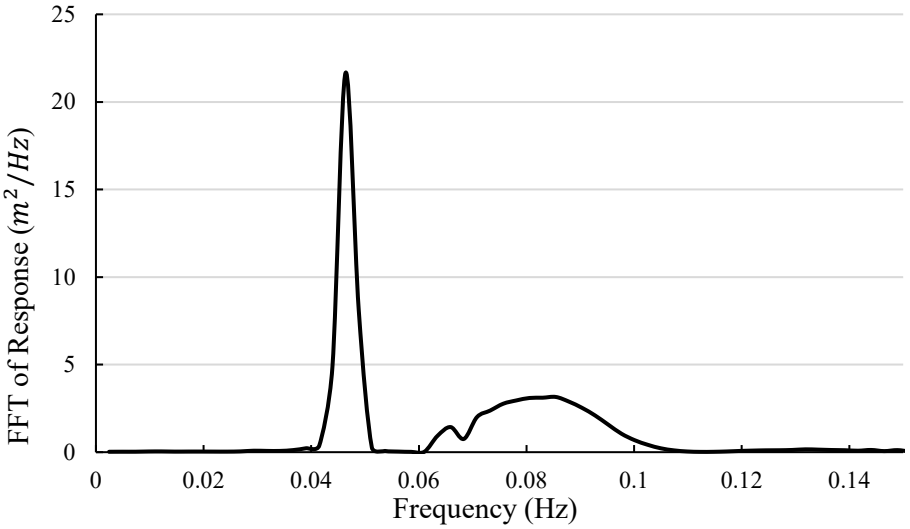

Fig. 12. Heave response without TLCD.

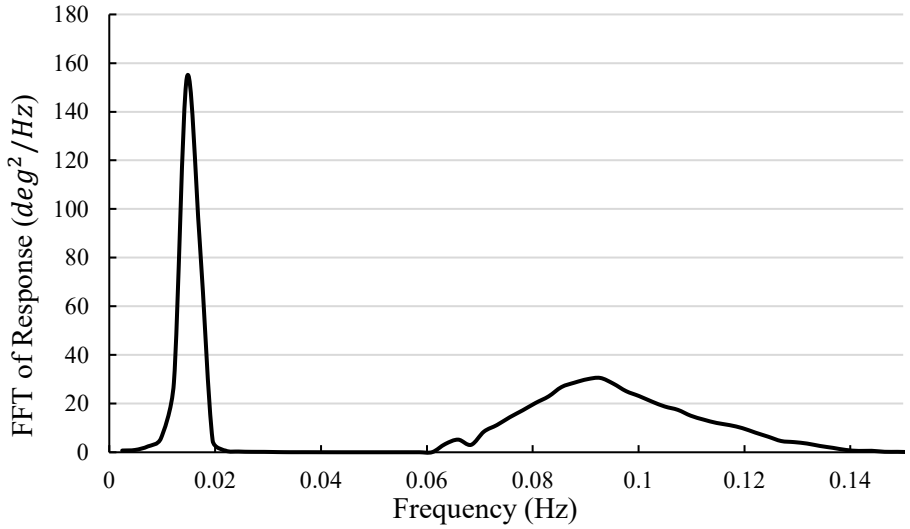

Fig. 13. Pitch response without TLCD

Comparing the fast Fourier transformed response of the structure with and without a TLCD, shows that there are no significant changes in the surge and heave motions. However, a considerable decrease can be seen for the pitch motion in the range of the natural frequency of the platform, but no decrease occurs at the wave frequency motion.

Liquid fluctuation in the TLCD and the resulting forces are dominated by platform motion, which excites the damper; thus, most of the damper forces

are generated at low frequencies in accordance with the platform motion. By contrast, the wave force is accumulated at the wave frequencies where the damper force is negligible. This is why the effect of the TLCD on platform motion is significant only at low frequencies.

In order to explain the aforementioned phenomenon, wave induced forces and moments are compared with TLCD induced ones in Fig. 13 to Fig. 18 .The fast Fourier transformed forces and moments are displayed in these figures in wave-frequency and low-frequency ranges separately. It can be seen that in wave-frequency range, TLCD induced forces are negligible in comparison with wave induced ones. In low frequencies (near the natural frequency of the platform) TLCD induced moments are dominated in pitch motion. But in surge and heave motions, again wave induced forces are dominated.

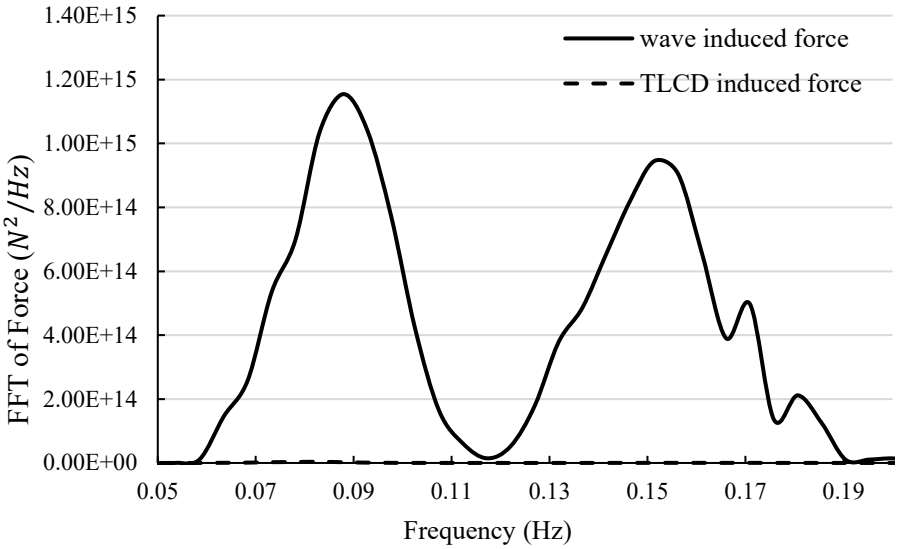

Fig. 14. Wave-frequency forces in surge direction

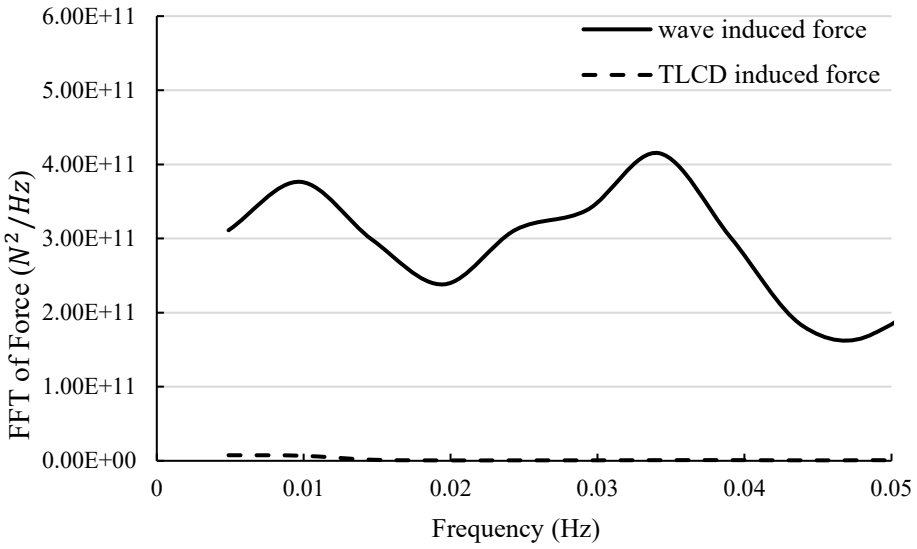

Fig. 15. Low-frequency forces in surge direction

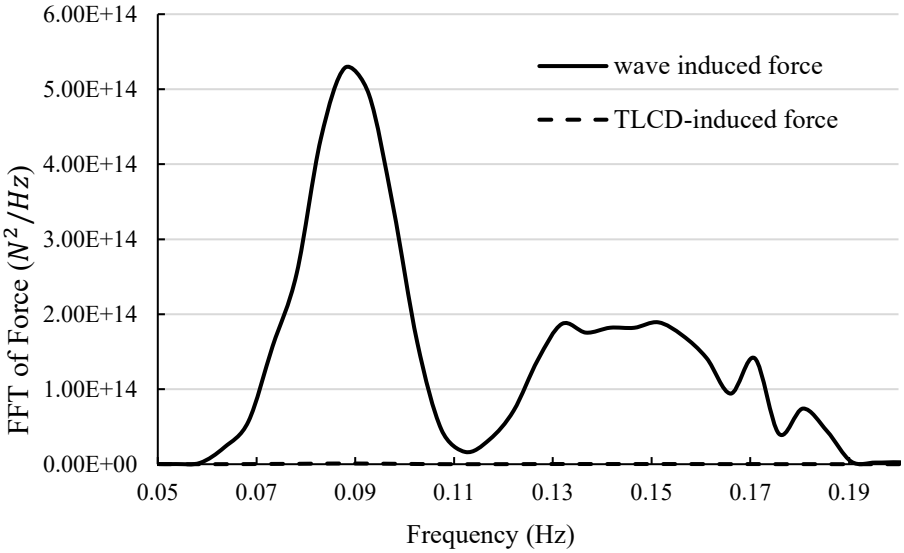

Fig. 16. Wave-frequency forces in heave direction

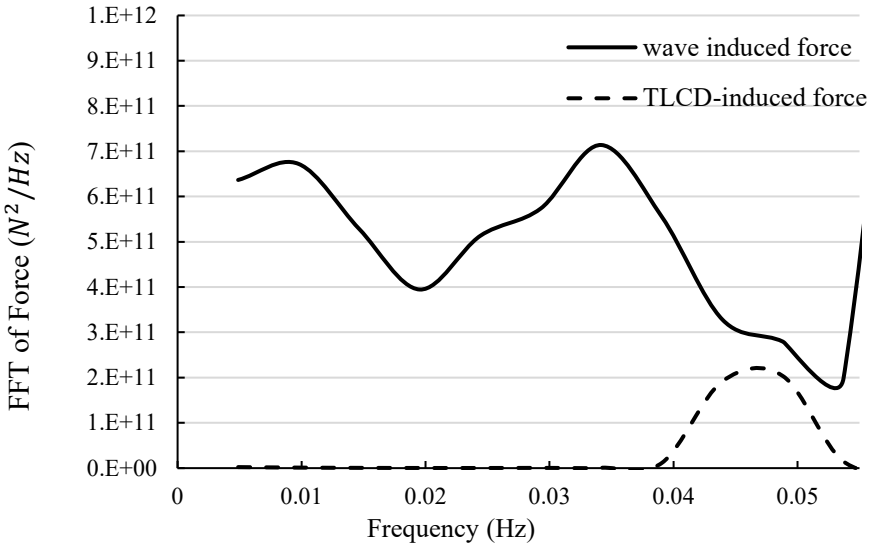

Fig. 17. Low-frequency forces in heave direction

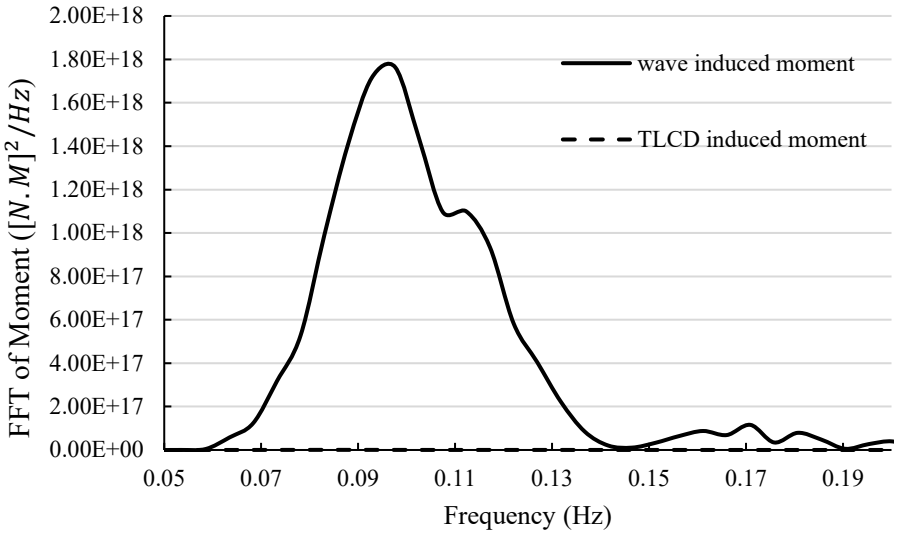

Fig. 18. Wave-frequency moment in pitch direction

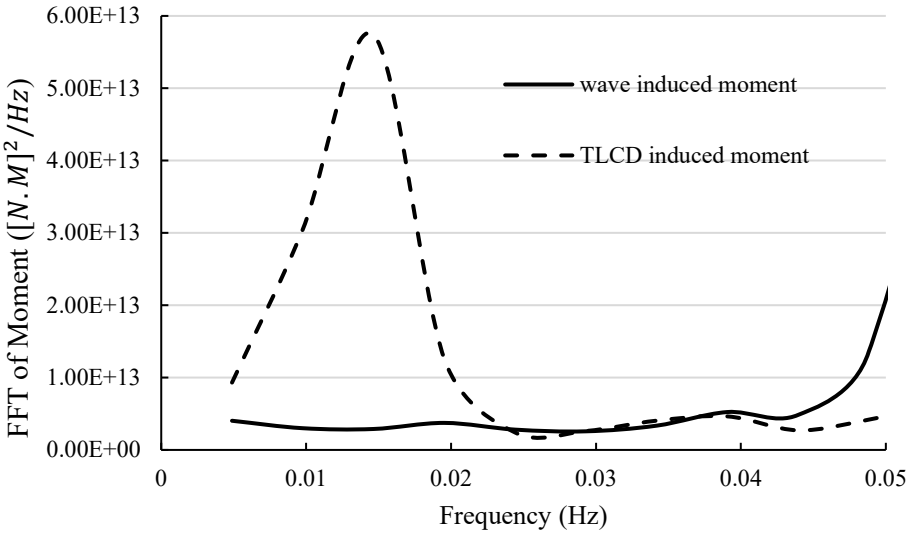

Fig. 19. Low-frequency moment in pitch direction

In the following sections, only results of pitch motion are presented, as no reduction is achieved in the surge and heave motions with a TLCD. For this reason, the pitch motion results are shown in the low frequency range, where the effect of the TLCD on platform motion is shown to be considerable.

4.1. Parametric analysis of platform response

4.1.1. Variation of head loss coefficient (ξ)

Table 3 lists four values for the head loss coefficient as they are related to the different blocking ratios of the TLCD orifice. These values are 3.5, 5.5, 12.5 and 55 for blocking ratios of 20%, 40%, 60% and 80%, respectively. The resultant FFT transformed responses are shown in Fig. 19. It can be seen that, for the case under study, the platform pitch motion is not affected by the damper when the blocking ratio does not exceed 40%. Beyond that, the damper efficiency increased as the blocking ratio of the damper orifice is increased up to 80%.

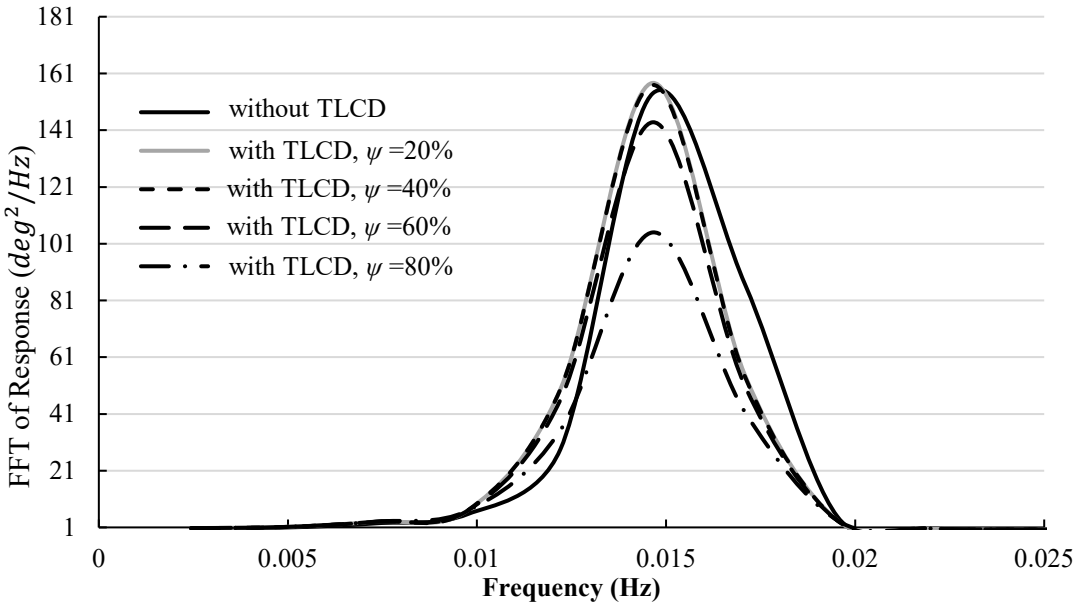

Fig. 20. Low-frequency pitch response vs. TLCD head loss coefficient.

4.1.2. Variation of natural frequency (f_{TLCD})

The TLCD frequency affects its efficiency and it is recommended to be equal to the natural frequency of the main structure [12,18,40]. However, it is not possible to tune the damper as recommended because of the dimensions of the floating platform and TLCD. At $A_v/A_h = 1$, the equivalent length of the liquid in the damper (L_{eq}) is limited to 85 m. This results in a frequency of 0.077 Hz (T = 13.07 sec) with a platform frequency of about 0.015 for pitch motion. An increase in A_v/A_h to 5.76 decreases the damper frequency to about 0.038 Hz, which is still about three times the platform frequency.

Fig. 20 shows the low-frequency response of a platform with a TLCD at different natural frequencies.

Although the frequency of the TLCD is far higher than that of the platform, it is apparent that damper efficiency is increased with decreasing the tuning ratio ($f_{TLCD}/f_{Structure}$) to 1.

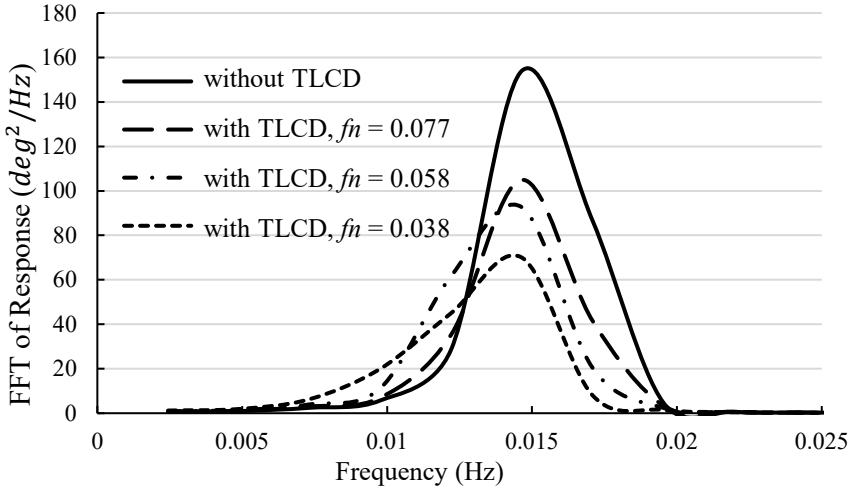

Fig. 21. Pitch low-frequency response vs. TLCD natural frequency.

4.1.3. Platform-TLCD mass ratio

Gao et al. [12] stated that, the mass ratio should be less than 2% for civil engineering applications. However, Wu et al. [18] have presented design guidelines for TLCDs with mass ratios of up to 5%. Chatterjee and Chakraborty [40] studied TLCD mass ratios of up to 14%. In the present research, the mass ratio is varied from 0.08% to 19%, as greater ratios are not practical. It is appropriate to use a small mass ratio to determine the maximum efficiency of a TLCD. Fig. 21. The Abbreviation *MR* is defined for the mass ratio in this figure. shows the effect of TLCD mass ratio on the platform response. The efficiency of damper is denoted as the "motion reduction factor" and is defined as the percentage of decrease in the significant double amplitude of the platform response. Fig. 22 shows the motion reduction factor versus the TLCD mass ratio. As seen, the TLCD efficiency is increased by increasing the mass ratio up to 10%. Beyond that, the damper efficiency is deteriorated. This means that the optimum mass ratio of the damper of the floating platform is about 10%.

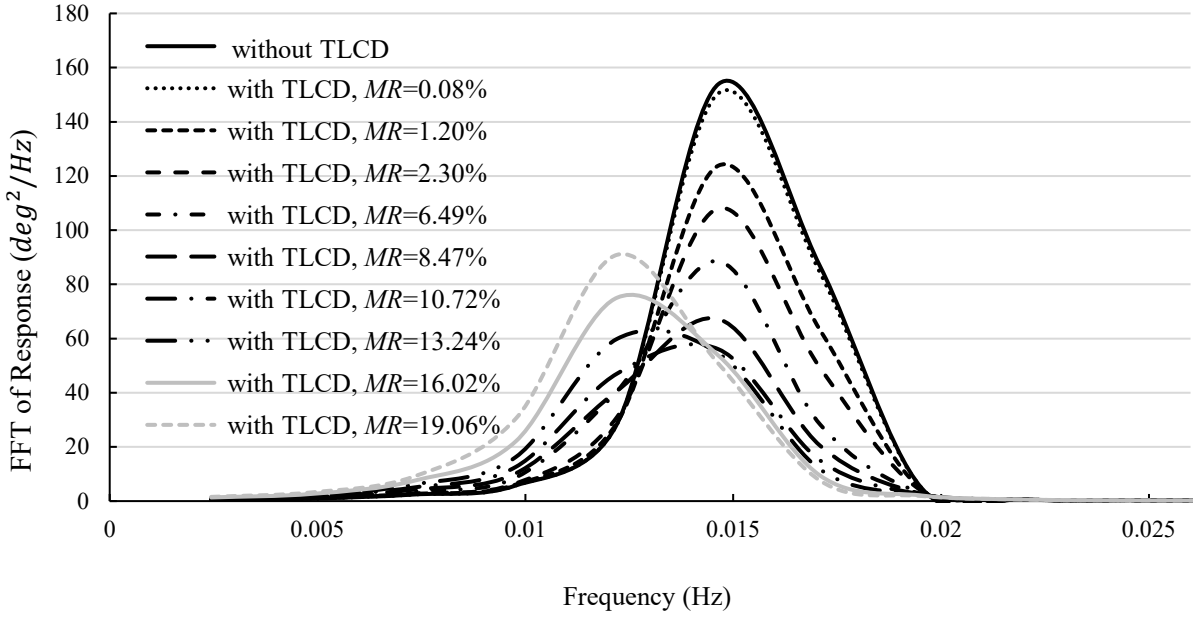

Fig. 22. Pitch low-frequency response vs. structure-TLCD mass ratio.

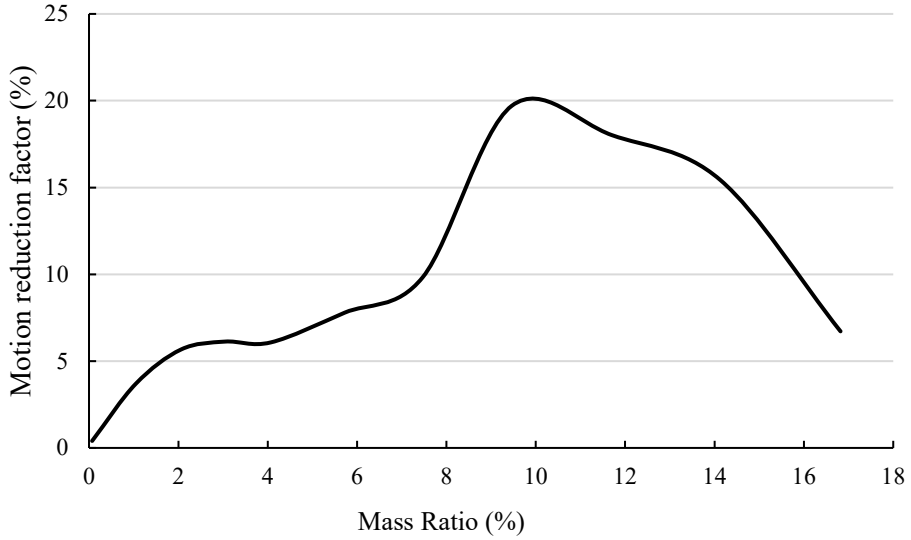

Fig. 23. Effect of TLCD mass ratio on motion reduction factor.

4.2. Effect of excitation term on TLCD function

As described in section 2, the terms on the right-hand side of Eq.(2.13) represent the effect of the motion of the structure-TLCD system on liquid fluctuation in the TLCD. The first three terms denote the pure horizontal, vertical and rotational motions. These variables are compared to determine the effect of platform motion at different DOF values on TLCD excitation. Values of additional terms are also compared to determine their effect on damper excitation.

In Eq.(2.13), the excitation terms are sensitive to the width of the TLCD (B), the length of the liquid in the tube (L) and the vertical distance of the rotating center from the horizontal tube (D). These parameters are kept constant in this parametric study. The excitation terms are compared at an optimum mass ratio of 10% and the results are depicted in Fig. 23. It can be seen that the X-term and θ-term for the surge and pitch motions of the platform have significant effects on TLCD excitation. The Z-term and additional terms show very small values when compared with those of the X-term and θ-term. It could be concluded that, the Z-term and additional terms have little influence on damper excitation for the GVA4000 in the defined wave condition.

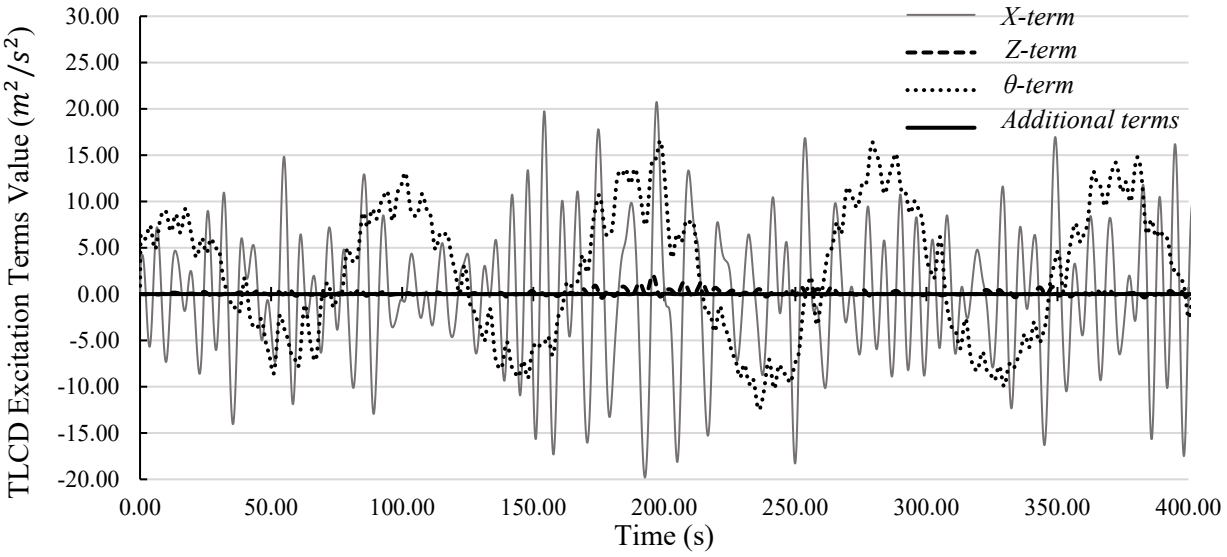

Fig. 24. Excitation terms induced by GVA4000 motion in TLCD governing equation.

The effect of rotational motion is neglected in previous studies, including those by Lee et al. [19], who studied the application of TLCDs to TLPs. It would be a suitable simplification method, because TLPs show high stiffness values in the heave and pitch directions, which lead to relatively slight motion [41]. In comparison with TLPs, semisubmersibles show much larger rotational motion [41]; thus, it may not be appropriate to ignore the effect of the rotational motion of a semisubmersible on TLCD excitation.

4.3. Effect of additional terms in governing equation of TLCD

Numerical modeling is performed again to determine the effect of the inclusion of the additional terms in the TLCD governing equation. Here, the additional terms are omitted from Eq.(2.13) and only the *X*-term, *Z*-term and θ-term are considered when calculating the motion of the liquid in the TLCD. The results are almost identical to those from the previous stage. No considerable effect is observed on the wave-frequency motion of the platform and the platform response in the surge and heave directions is not affected by the damper.

Because the results are very similar in the presence and absence of the additional terms, it is difficult to recognize the differences between the FFT transformed response diagrams.

Table 4 provides the computed motion reduction factors to allow better comparison of the results. It can be seen that the resultant reduction factors for both cases have negligible differences. This means that the inclusion of additional terms in the governing equation for TLCD has no effect on its efficiency.

Table 4. Effect of TLCD on platform motion with and without additional terms in governing equation

	TLCD characteristics			Motion reduction factor (%)	
Selected specification of TLCD for parametric study	T (s)	Mass ratio (%)	Head loss coefficient (ξ)	With additional terms	Without additional terms
Head loss Coefficient	13.07	3.44	3.50	0.5807	0.5912
			5.50	0.6731	0.6605
			12.50	2.0409	2.0052
			55.00	6.1200	6.1458
Natural frequency (period)	13.07	3.44	55.00	6.1247	6.1132
	17.36			6.5431	6.6217
	26.42			9.5438	9.5914
TLCD/structure mass ratio	13.07	0.08	55.00	0.4031	0.4218
		1.2		3.7033	3.6502
		2.3		5.6701	5.6600
		6.49		7.7883	7.7741
		8.47		9.8447	9.8211
		10.72		19.7032	19.7255
		13.24		18.0207	18.0410
		16.02		15.4323	15.4412
		19.06		6.7105	6.734

4.4. Effect of rotational motion of platform on TLCD function

The effect of the rotational motion of the platform on TLCD function is determined using a numerical model without the θ-term in Eq.(2.13). The responses then are compared with those in which the rotational motion of the platform is taken into account (with θ-term in Eq. (2.13)). The motion reduction factors are compared in Fig. 24 with and without the θ-term. As seen, a 40% amplification is obtained for a mass ratio of 0.9% which is not a reasonable result. Increasing the mass ratio to 2% results in decreasing the platform motion rapidly by 50%. It is evident that the results are unreliable when the effect of platform rotation on TLCD is ignored; thus, it is necessary to consider the effect of the rotational motion of the platform on TLCD excitation.

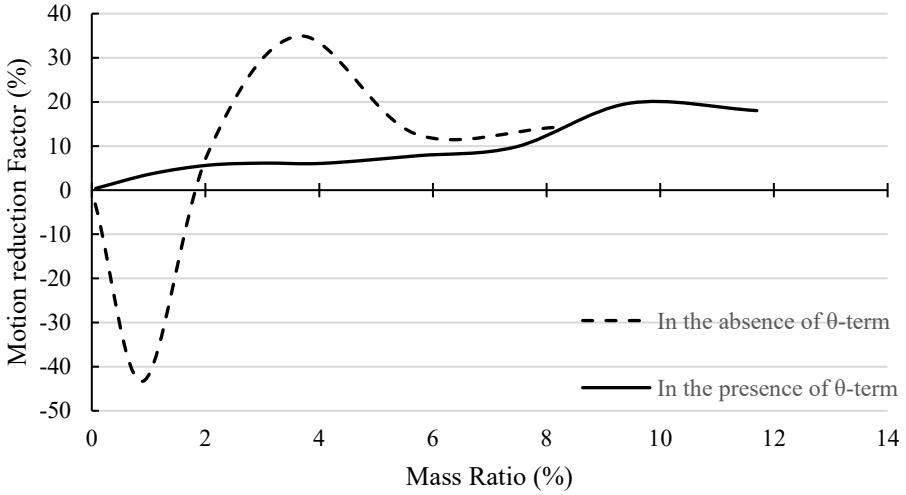

Fig. 25. TLCD mass ratio vs. motion reduction factor with and without *θ*-term.

5. Conclusions

A numerical study is carried out to investigate the effect of a tuned liquid column damper (TLCD) on the motion reduction of a semisubmersible platform. The simultaneous effect of the transitional and rotational motions of the platform on TLCD function are taken into account by deriving an appropriate formula. By time domain analysis method, linear and nonlinear wave forces as well as wave-frequency and low-frequency motions of the platform are examined in irregular waves.

It is shown that separate equations for pure transition and rotation could be applied to take into account the combined transitional and rotational effects of the liquid fluctuation in the TLCD. It is also found that the rotation of the platform affects TLCD function significantly.

This research also shows that only the low-frequency motion of a semisubmersible platform can be decreased with the use of a TLCD. A parametric study reveals that a value of 10% for the platform-damper mass ratio is optimal for the selected floating platform and increasing the blocking ratio of the damper orifice to 80% increases the efficiency of damper. It is also observed that, although the feasible frequency of the TLCD is far higher than the natural frequency of the semisubmersible, decreasing the damper frequency increases the efficiency.

6. References

1- G.F. Clauss, L. Birk, (1996), *Hydrodynamic shape optimization of large offshore structures*, Appl. Ocean Res., Vol.18, p.157–171.

2- M. Adjami, M. Shafieefar, (2008), *Hydrodynamic shape optimization of semi-submersibles using a genetic algorithm*, J. Mar. Sci. Technol., Vol.16, p.109–122.

3- J.Y. Lee, S.J. Lim, (2008), *Hull Form Optimization of a Tension-Leg Platform Based on Coupled Analysis*, Proc. Eighteenth Int. Offshore Polar Eng. Conf., Vol.8, p.100–107.

4- M. Muskulus, S. Schafhirt, (2014), *Design optimization of wind turbine support structures-A review*, J. Ocean Wind Energy, Vol.1, p.12–22.

5- M. Hall, B. Buckham, C. Crawford, (2014), *Hydrodynamics-based floating wind turbine support platform optimization: A basis function approach*, Renew. Energy, Vol.66, p.559–569.

6- M. Shafieefar, A. Rezvani, (2007), *Mooring optimization of floating platforms using a genetic algorithm*, Ocean Eng., Vol.34, p.1413–1421.

7- M. Mirzaei, (2014), *Mooring Pattern Optimization Using A Genetic Algorithm*, J. Teknol., Vol.2, p.189–193.

8- N. Ren, Y. Li, J. Ou, (2012), *The effect of additional mooring chains on the motion performance of a floating wind turbine with a tension leg platform*, Energies, Vol.5, p.1135–1149.

9- M. Brommundt, L. Krause, K. Merz, M. Muskulus, (2012), *Mooring system optimization for floating wind turbines using frequency domain analysis*, Energy Procedia, Vol.24, p.289–296.

10- R. Kandasamy, F. Cui, N. Townsend, C.C. Foo, J. Guo, A. Shenoi, Y. Xiong, (2016), *A review of vibration control methods for marine offshore structures*, Ocean Eng., Vol.127, p.279–297.

11- A. Di Matteo, A. Pirrotta, F. Lo Iacono, G. Navarra, (2012), *The Control Performance of TLCD and TMD : Experimental Investigation*, 5th Eur. Conf. Struct. Control, p.1–9.

12- H. Gao, K.C.S. Kwok, B. Samali, (1997), *Optimization of tuned liquid column dampers*, Eng. Struct., Vol.19, p.476–486.

13- A. Kareem, T. Kijewski, Y. Tamura, (2007), *Mitigation of Motion of Tall Buildings with*

Specific Examples of Recent Applications, Wind Struct., p.201–251.

14- B. Samali, K.C.S. Kwok, D. Tapner, Vibration control of structures by tuned liquid column dampers, in: Proc., IABSE, 14th Congr., 1992: pp. 461–466.

15- A. Ghosh, B. Basu, (2004), *Seismic vibration control of short period structures using the liquid column damper*, Eng. Struct., Vol.26, p.1905–1913.

16- T. Balendra, C.M. Wang, G. Rakesh, (1999), *Effectiveness of TLCD on various structural systems*, Eng. Struct., Vol.21, p.291–305.

17- C.C. Chang, (1999), *Mass dampers and their optimal designs for building vibration control*, Eng. Struct., Vol.21, p.454–463.

18- J.C. Wu, M.H. Shih, Y.Y. Lin, Y.C. Shen, (2005), *Design guidelines for tuned liquid column damper for structures responding to wind*, Eng. Struct., Vol.27, p.1893–1905.

19- H.H. Lee, S.H. Wong, R.S. Lee, (2006), *Response mitigation on the offshore floating platform system with tuned liquid column damper*, Ocean Eng., Vol.33, p.1118–1142.

20- F. Sakai, S. Takaeda, T. Tamaki, Tuned liquid column damper-new type device for suppression of building vibration, in: Int. Conf. High-Rise Build., 1989: pp. 926–31.

21- X. Zeng, Y. Yu, L. Zhang, Q. Liu, H. Wu, (2014), *A New Energy-Absorbing Device for Motion Suppression in Deep-Sea Floating Platforms*, Energies, Vol.8, p.111–132.

22- H.H. Lee, H.H. Juang, (2012), *Experimental study on the vibration mitigation of offshore tension leg platform system with UWTLCD*, Smart Struct. Syst., Vol.9, p.71–104.

23- C. Coudurier, O. Lepreux, N. Petit, (2018), *Modelling of a tuned liquid multi-column damper. Application to floating wind turbine for improved robustness against wave incidence*, Ocean Eng., Vol.165, p.277–292.

24- C. Holden, T. Perez, T.I. Fossen, (2011), *A Lagrangian approach to nonlinear modeling of anti-roll tanks*, Ocean Eng., Vol.38, p.341–359.

25- M. Shadman, A. Akbarpour, (2012), *OMAE2012-83330*, p.1–7.

26- M. Shahrabi, K. Bargi, (2019), *Enhancement the Fatigue Life of Floating Breakwater Mooring System Using Tuned Liquid Column Damper*, Lat. Am. J. Solids Struct., Vol.16,.

27- M.J. Hochrainer, (2005), *Tuned liquid column damper for structural control*, Acta Mech., Vol.175, p.57–76.

28- S.D. Xue, J.M. Ko, Y.L. Xu, (2000), *Tuned liquid column damper for suppressing pitching motion of structures*, Eng. Struct., Vol.22, p.1538–1551.

29- X. Suduo, J.M. Ko, Y.L. Xu, (2002), *Wind-induced vibration control of bridges using liquid column damper*, Vol.1, p.271–280.

30- A.A. Taflanidis, D.C. Angelides, G.C. Manos, (2005), *Optimal design and performance of liquid column mass dampers for rotational vibration control of structures under white noise excitation*, Eng. Struct., Vol.27, p.524–534.

31- H. Sabziyan, H. Ghassemi, F. Azarsina, S. Kazemi, (2014), *Effect of Mooring Lines Pattern in a Semi-submersible Platform at Surge and Sway Movements*, J. Ocean Res., Vol.2, p.17–22.

32- C.C. Chang, C.T. Hsu, (1998), *Control performance of liquid column vibration absorbers*, Eng. Struct., Vol.20, p.580–586.

33- G.F. Clauss, C.E. Schmittner, K. Stutz, (2002), *Time-domain investigation of a semisubmersible in rogue waves*, 21st Int. Conf. Offshore Mech. Arct. Eng.,.

34- N.M. Newmark, (1959), *A method of computation for structural dynamics*, J. Eng. Mech. Div., Vol.85, p.67–94.

35- M. López, F. Taveira-Pinto, P. Rosa-Santos, (2017), *Numerical modelling of the CECO wave energy converter*, Renew. Energy, Vol.113, p.202–210.

36- K.C. Subrata, S. Cliakrabarti, Handbook of offshore engineering, 2005.

37- ANSYS, Aqwa Theory Manual, 2013.

38- A.P.I. RP2A-WSD, Recommended practice for planning, designing and constructing fixed offshore platforms--working stress design--, 2014.

39- M. Keddam, (2002), *Offshore Hydromechanics*, Electrochim. Acta, Vol.47, p.1503–1504.

40- T. Chatterjee, S. Chakraborty, (2014), *Vibration mitigation of structures subjected to random wave forces by liquid column dampers*, Ocean Eng., Vol.87, p.151–161.

41- B. Li, K. Liu, G. Yan, J. Ou, (2011), *Hydrodynamic comparison of a semi-submersible, TLP, and Spar: Numerical study in the South China Sea environment*, J. Mar. Sci. Appl., Vol.10, p.306–314.